# Investigating the Effect of the Injector Length/Diameter ratio on the Primary Breakup of Liquid Jets using X-ray Diagnostics

A. R. Osta, J. Lee, K. A. Sallam*
Oklahoma State University, Stillwater, Oklahoma 74078, USA

K. Fezzaa
Advanced Photon Source, Argonne National Laboratory, Argonne, Illinois 60439, USA

**Abstract**

An investigation of the disintegration of turbulent liquid jets in gases was carried out by using x-ray diagnostics on injectors with a smooth entry (to eliminate cavitation) followed by straight passage with length-to-diameter ratio of 10 and 40. The test matrix is designed to maintain the same aerodynamic forces in order to isolate the effects of jet turbulence on the breakup process. The tests were conducted at the Advanced Photon Source (APS) facility of Argonne National Laboratory. The x-ray source at the APS has a unique combination of properties such as high brilliance, small size, broad energy spectrum and flexible time structure (hybrid-singlet mode). This allows the surface and internal topography of fuel jets to be visualized and the breakup mechanism in the dense-spray near-injector region to be revealed. The present x-ray images revealed the presence of bubbles near the ligaments formation locations when the jet was injected in sub-atmospheric pressure. These bubbles were absent when the jet was injected at atmospheric pressure, however. The present results also show that the separation distance of the ligaments is influenced by the ligament sizes; the larger the ligament the further away its neighbors.

## Introduction

The disintegration of turbulent liquid jets in gases, a process termed turbulent primary breakup, has many industrial applications, especially in liquid fuel injection systems. Previous studies [1-3] have shown that the jet turbulent primary breakup processes were significantly influenced by the geometry of the injector passage. The dense spray core, however, is optically challenging to almost all of the standard visualization techniques. In order to visualize the changes undergone inside the jet core as well as in the dense near jet-exit region penetrating x-rays are more adequate probe. The APS undulator source produces a highly brilliant and collimated x-ray beam in a wide energy range (1-100 keV). This allows for a high-speed and high resolution visualization of the surface and internal structure of the liquid jet, and for the breakup mechanism in the dense-spray near-injector region to be revealed. Recently, Lin et al. [4] experimentally investigated near field structure of liquid jets in still air using double-pulse x-ray phase contrast imaging. Their images suggested that the effect of turbulence eddies within a liquid jet on its primary breakup in still air should be studied more. An intriguing question is the relative importance of the liquid turbulence and the aerodynamic forces in the breakup processes of fuel injection. The objective of the present study was to find an answer to this question by increasing the jet turbulence while maintaining the same level of aerodynamic forces along the jet surface. The present test matrix included testing two injectors with a smooth entry (to minimize cavitation) with length-to-diameter (L/D) ratio of 10, and 40, and the same injection velocity in order to isolate the effects of jet turbulence due to the nozzle passage length on the jet breakup process.

## Experimental Methods

The experimental apparatus is illustrated in Fig. 1. The turbulent round liquid jet was injected vertically downward using a pressure feed system into a collecting bucket. The test liquid was contained within a cylindrical stainless steel chamber. The nozzles had a smooth rounded entrance (R/D = 1.2) followed by round constant area passages having length-to-diameter ratios of 10 and 40 to provide different degrees of turbulence development at the jet exit. The liquid was forced through the nozzle by admitting high pressure air from a pressurized air tank to the top of the chamber through a solenoid valve. A baffle at the air inlet prevented undesirable mixing between the air and the test liquid.

The experiments were carried out at XOR 32-ID beamline of the APS. The undulator source provided the high X-ray brilliance necessary for this white-beam ultra-fast imaging technique. With the undulator gap set to 20 mm,

*Corresponding author, khaled.sallam@okstate.edu.

most of the intensity was located within the first harmonic at 9 keV, with a peak brilliance of ~ $10^{19}$ ph/s/mrad$^2$/mm$^2$/ 0.1% BW, and a natural bandwidth of 0.3 keV FWHM. The sample stage was located 40 m downstream from the source. A fast scintillator crystal (LYSO:Ce, with a 40 ns decay time) converted the transmitted X-rays into visible light (434nm). The sample-scintillator distance, set to 50 cm, corresponded to an optimized defocus value for Fresnel propagation contrast and spatial resolution. The images were captured with a fast CCD camera (Sensicam from Cooke Corp., 1024x1024 pixels and 6.7 μm pixel size) coupled to the scintillator via a microscope objective (X5, NA=0.14) and a 45º mirror. The effective pixel size was 1.3 μm, and the field of view of 1.3x1.7 mm$^2$ was matched to the available x-ray beam size. The pulsed nature of the x-ray beam combined with an adequate shuttering and timing of the setup provided an effective exposure time of 150 ps for each image.

In addition to some weak absorption effect, the contrast in the recorded images with this propagation-based imaging technique comes from a phase affect. After interaction with the sample, the x-rays wave field propagates in free space and its different components having been diffracted by the sample starts to overlap and interfere giving rise to a contrasted pattern. This contrast depends on the Laplacian of the phase shift undergone by the beam upon its passage through the sample [5]. As a consequence, this technique is most sensitive to boundaries and interfaces between materials with different refraction index or abrupt thickness variations, which are greatly enhanced [6]. Also, due to refraction and for the same interface, different curvatures will have very distinct "signature" contrasts. For instance, a bubble (gas surrounded by liquid) will have a dark/bright outer edge whereas a droplet (liquid surrounded by gas) will have an opposite boundary contrast (bright/dark) as illustrated in our simulations shown in Fig.2. When the jet was injected in sub-atmospheric pressure, there was a strong presence of bubbles near the location of the onset of ligaments as shown in Fig. 2. Those bubbles disappeared (although not completely) when the jet was injected in atmospheric pressure. Those bubbles are probably formed by dissolved air in the test liquid.

**Results and Discussion**

To visualize the breakup of the liquid jet in the near-injector regions, a spray map, as shown in Fig. 3, has been constructed with several high resolution images to overcome the small field of view used in the present study. By zooming on the surface topography obtained in the x-ray images as shown in Fig. 3.b and following their dynamics, measurements were made with respect to the ligaments sizes and their spatial distribution. The data reduction methods were similar to previous work on breakup of turbulent jets in still air [7]. Ligaments were approximated as cylinders and were represented by their average diameters. The ligament average diameter $d_{lig}$ is calculated by:

$$d_{lig} = A_{lig} / L_{lig} \tag{1}$$

where $L_{lig}$ is the ligament projected length and $A_{lig}$ is the ligament projected area on the image.

The ligament location on the *curved* jet surface, s, was calculated from the projected horizontal location, x, by:

$$S = R \sin^{-1}(x/R) \tag{2}$$

where R is the radius of the jet. The plot of the ligaments distribution along the streamwise direction is shown in Fig. 4 where the dashed gridlines mark the individual field of views of each x-ray image. It is hard to confirm whether the ligaments are formed along ridges because of the limited field of view of each image and more importantly because the ligaments located at both the front and the back surfaces are indistinguishable from the present x-ray images. In order to investigate the relationship between a ligament size and the separation distances with its neighbors, ligaments located at the right or the left edges were considered as shown in Fig. 5. The separation distance, L, between an edge ligament and its neighboring ligament, as shown in Fig. 5, is calculated by:

$$L = \sqrt{S^2 + y^2} \tag{3}$$

where y and s are the vertical and circumferential distance between those two ligaments, whether the neighboring ligament is located on the front or the back surface. The ligaments separation distance, L, is plotted in Fig. 6, vs. the size of the ligaments (edge ligament with diameter $d_1$ and its neighbors with diameter $d_2$) for the two injector tested in the present study. The results obtained so far show that there is a strong relation between the ligaments spacing and their sizes. The larger the ligament, the further its neighboring ligaments. This suggests that the creation of a ligament at a particular location reduce the amount of turbulent kinetic energy available to create more ligaments nearby.

In order to understand the rates of breakup, the present x-ray images were used to measure a surface breakup efficiency factor, $\varepsilon$, defined as follows:

$$\varepsilon = \Sigma\, n_i((\pi/4)d_{lig}^2)_i/A \quad (4)$$

where A is the surface of the jet and the limit $\varepsilon = 1$ represent conditions where ligaments are formed in continuous manner all over the liquid jet surface. The relatively large ligaments separation distances measured in the present study suggest that generally $\varepsilon << 1$. Present measurements for $\varepsilon$ is shown in Fig. 7 for the L/D = 10 and 40. The surface breakup efficiency factor is small for the two injectors as expected. The large scatter of the data due to the sampling limitation, however, renders the results for the two injectors indistinguishable. Further studies are needed to clarify if there an effect of the injector L/D ratio on the rates of breakup.

**Concluding remarks**

Highly energetic and penetrating x-rays beam was used to observe the ligaments sizes and distributions on turbulent liquid jets injected from two injectors with L/D= 40 and 10.

1. When the liquid jet was injected in an environment below atmospheric pressure, bubbles were observed near the locations of the onset of ligaments formation. These bubbles are most likely due to the dissolved gases in the test liquid.
2. The ligament sizes are correlated with their separation distances; the larger the ligament the further away its neighbors.
3. The surface breakup efficiency factor is very small due to the relatively large ligaments separation distances.

Finally, the large scatter of the data due to the sampling limitation, however, renders the results for the two injectors indistinguishable. Further measurements are needed to clarify if there is an effect of the injector L/D ratio on the rates of breakup.

**Acknowledgement**

Use of the Advanced Photon Source was supported by the U.S. Department of Energy, Office of Science, Office of Basic Energy Sciences, under Contract No. DE-AC02-06CH11357.

**Nomenclature**

| | | |
|---|---|---|
| $d_j$ | = | *Liquid jet diameter at jet exit* |
| $D$ | = | *Inner diameter of the nozzle* |
| $L$ | = | *Length of the nozzle passage* |
| $Oh$ | = | *Ohnesorge number,* $\mu_L/(\rho_L d_j \sigma)^{1/2}$ |
| $Re_{LD}$ | = | *Liquid jet Reynolds number,* $(\rho_L v_j d_j/\mu_L)$ |
| $t$ | = | *Time* |
| $v$ | = | *Stream wise velocity (in the vertical direction)* |
| $x$ | = | *Projected length along the diameter* |
| $y$ | = | *Downstream distance (vertical)* |
| $R$ | = | *Radius* |

**Subscripts**

| | | |
|---|---|---|
| $b$ | = | *Base of the ligament* |
| $j$ | = | *Jet exit property* |
| $lig$ | = | *Ligament properties.* |

**References**

1. McCarthy, M. J., and Molloy, N. A., *The Chemical Engg. Journal*, 7:1-21 (1974).
2. Karasawa, T., Tanaka, M., Abe, K., Shiga, S., Kurabayashi, T., *Atomization and Sprays* 2:411-426 (1992).
3. Wu, P.-K., Miranda, R. F., and Faeth, G. M., *Atomization and Sprays* 5:175-196 (1995).
4. Lin, K. C., Carter, C., Fezzaa, K., and Wang, J., 21st Annual Conference on Liquid Atomization and Spray Systems, Orlando, Florida, May 2008.
5. Guigay J. P., Langer M., Boistel R., and Cloetens P., *Opt. Lett.* 32, 1617-1619 (2007).
6. Wilkins, S. W., Gureyev, T. E., Gao, D., Pogany, A., and Stevenson, A. W., *Nature* 384:335–338 (1996).
7. Sallam, K. A., and Faeth, G. M., *AIAA Journal* 41:1514-1524 (2003).

**Table 1.** Test conditions

| **Parameters** | |
|---|---|
| Nozzle diameter (m) | 0.004 |
| Nozzle entrance curvature (R/D) | 1.2 |
| Nozzle passage length (L/D) | 10, 40 |
| Density of gas, air ($\rho_{air}$) – kg/m$^3$ | 1.215 |
| Dynamic viscosity of gas, air ($\mu_{air}$) - Ns/m$^2$ | 1.85E-05 |
| Surface tension of test liquid, water ($\sigma_w$) – N/m | 0.0708 |
| Density of test liquid, water. ($\rho_w$)-kg/m$^3$ | 997 |
| Dynamic viscosity of test liquid ($\mu_w$) – Ns/m$^2$ | 8.94E-04 |
| Jet Weber Number ($We_{LD}$) | 50,700 |
| Jet Velocity ($V_j$) – m/s | 30 |
| Jet Reynolds Number ($Re_{LD}$) | 134,000 |
| Ohnesorge Number (Oh) | 0.0017 |

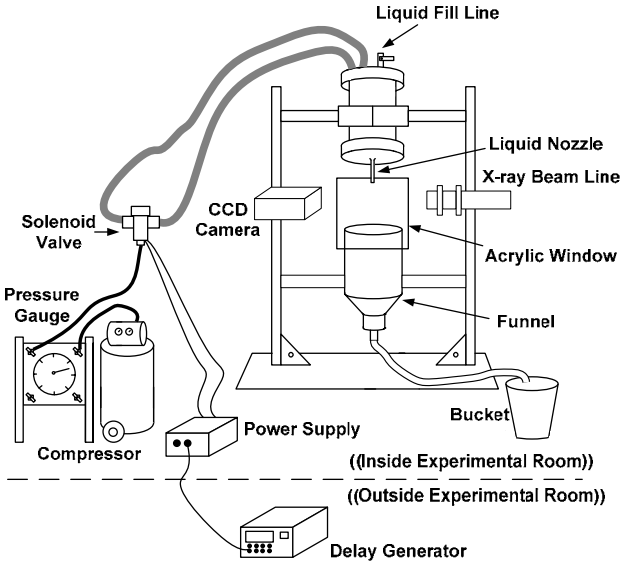


**Figure 1.** Experimental apparatus.

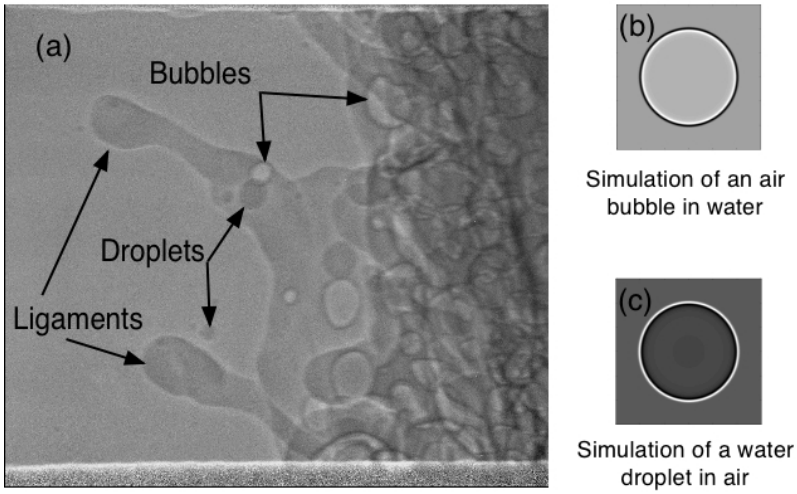


**Figure 2.** A typical X-ray image of the jet showing (a) the surface ligaments and the bubble entrainment in the jet. (b, c) are simulations of a bubble and a drop respectively

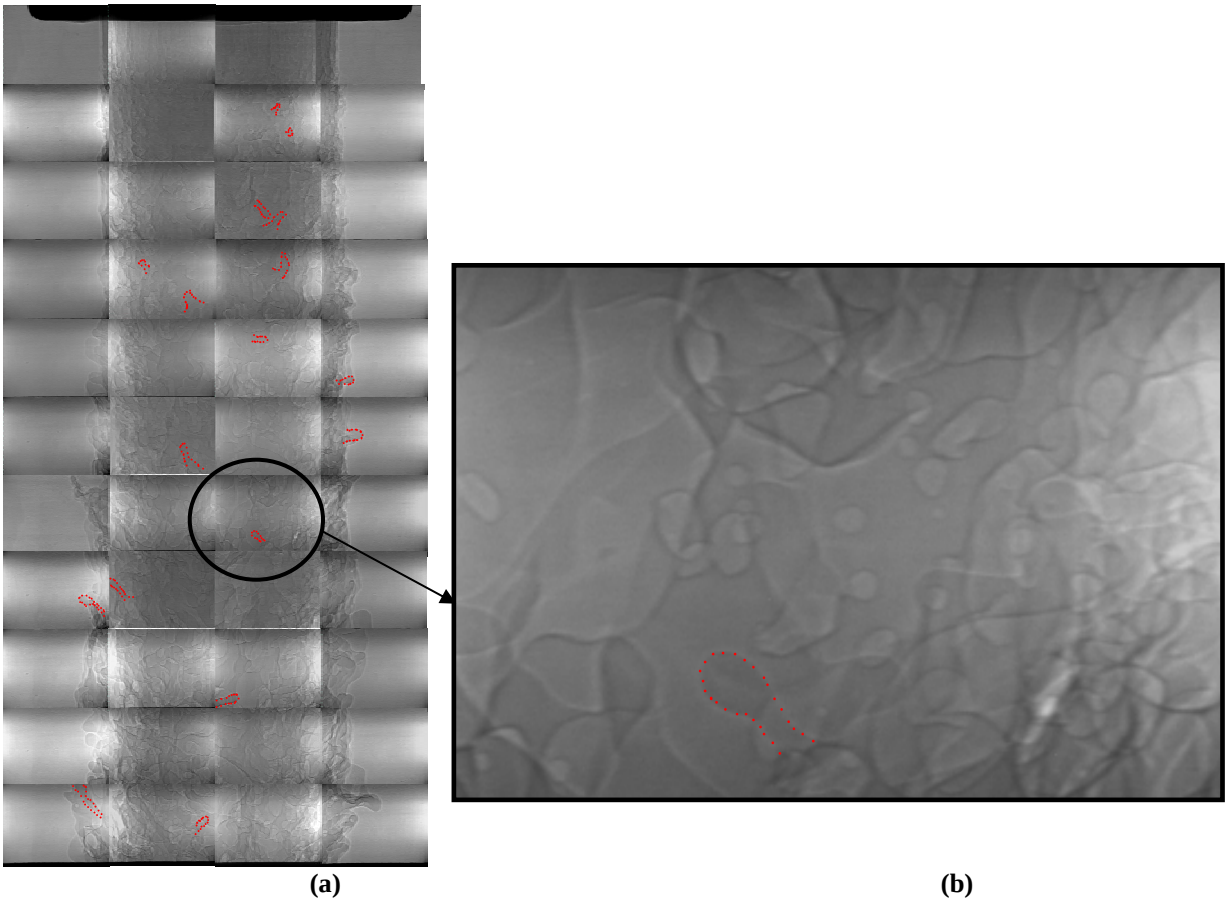


**Figure 3.** Liquid jet breakup for L/D = 40. (a) map patched with high resolution x-ray images showing examples of spotted ligaments. (b) Zoom-in image with the edge of a ligament outlined in red dots.

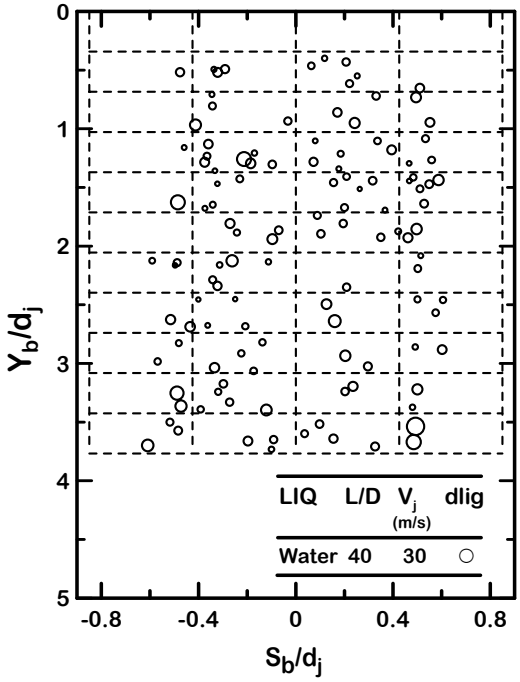


**Figure 4.** Ligament spatial distribution for L/D = 40, for both the front and the back faces.

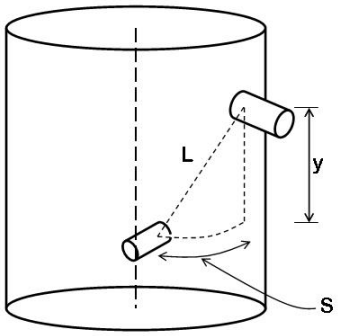


**Figure 5.** Cartoon of the separation distance between an "edge" ligament and its neighboring ligament.

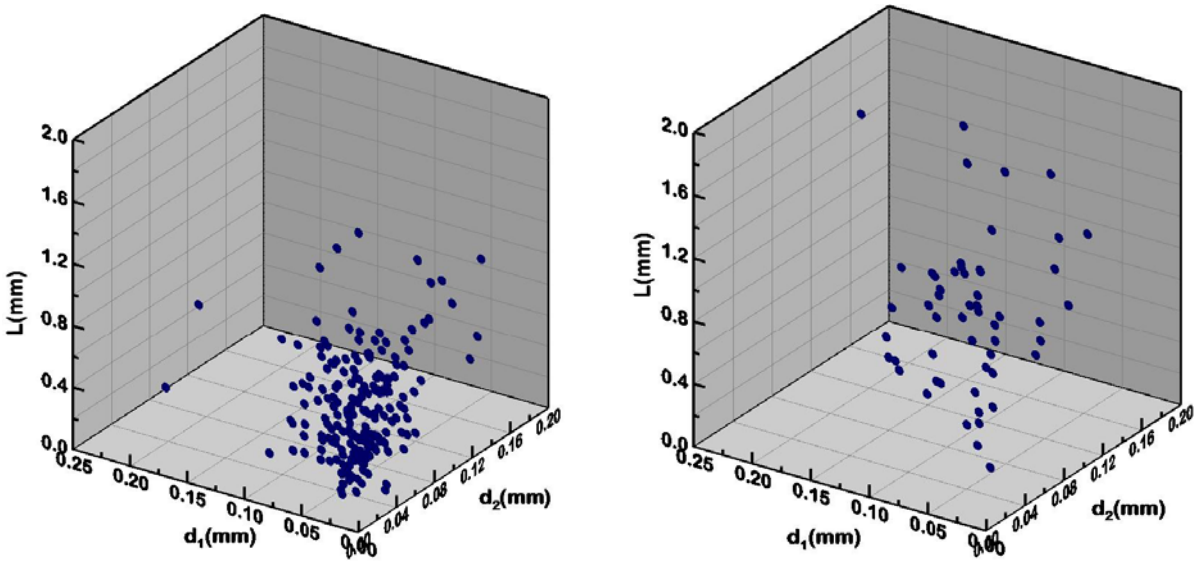


**Figure 6.** Ligament separation plot for D = 4mm and (a) L/D = 10, (b) L/D = 40.

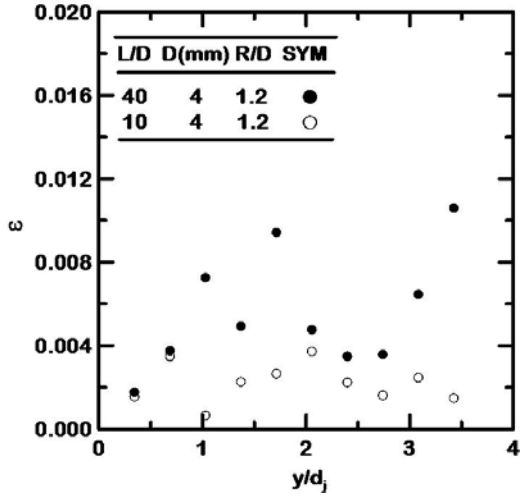


**Figure 7.** Surface efficiency parameter near the onset of breakup.